LBL-20698
Preprint

Lawrence Berkeley Laboratory

UNIVERSITY OF CALIFORNIA

Materials & Molecular Research Division

RECEIVED
LAWRENCE BERKELEY LABORATORY
MAR 2 1987
LIBRARY AND
DOCUMENTS SECTION

Submitted to Journal of Applied Physics

ON THE GRAIN BOUNDARY PHASE IN IRON-RARE EARTH-BORON MAGNETS

R. Ramesh, J.K. Chen, and G. Thomas

September 1986

TWO-WEEK LOAN COPY
This is a Library Circulating Copy
which may be borrowed for two weeks

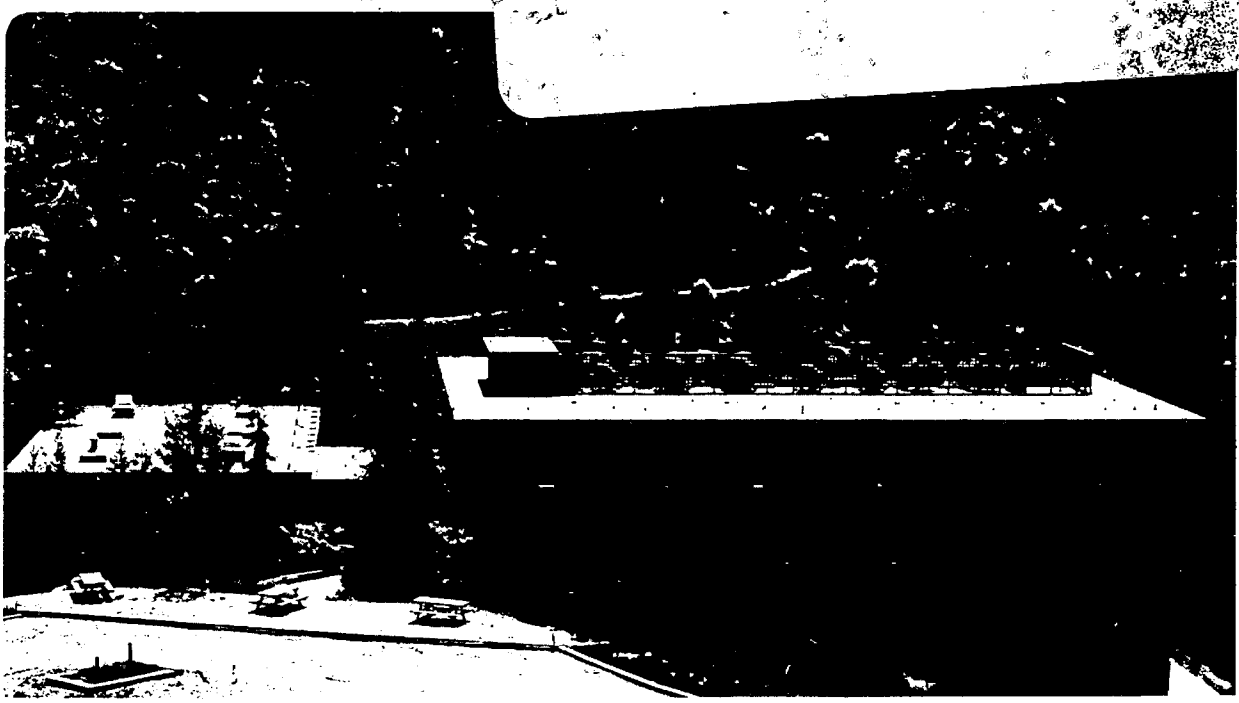

LBL-20698 c.2

Prepared for the U.S. Department of Energy under Contract DE-AC03-76SF00098

DISCLAIMER

This document was prepared as an account of work sponsored by the United States Government. While this document is believed to contain correct information, neither the United States Government nor any agency thereof, nor the Regents of the University of California, nor any of their employees, makes any warranty, express or implied, or assumes any legal responsibility for the accuracy, completeness, or usefulness of any information, apparatus, product, or process disclosed, or represents that its use would not infringe privately owned rights. Reference herein to any specific commercial product, process, or service by its trade name, trademark, manufacturer, or otherwise, does not necessarily constitute or imply its endorsement, recommendation, or favoring by the United States Government or any agency thereof, or the Regents of the University of California. The views and opinions of authors expressed herein do not necessarily state or reflect those of the United States Government or any agency thereof or the Regents of the University of California.

ON THE GRAIN BOUNDARY PHASE IN IRON-RARE EARTH-BORON MAGNETS

R.RAMESH, J.K.CHEN and G.THOMAS
DEPARTMENT OF MATERIALS SCIENCE AND MINERAL ENGINEERING AND MATERIALS AND MOLECULAR RESEARCH DIVISION AND NATIONAL CENTER FOR ELECTRON MICROSCOPY, LAWRENCE BERKELEY LABORATORY, UNIVERSITY OF CALIFORNIA, BERKELEY, CA 94720.

ABSTRACT: Results of structural and microanalytical studies on sintered Iron-Rare Earth-Boron permanent magnets are presented in this paper. It is shown that the structure of the phase present at the two grain boundaries is the same as that of the phase at the triple grain junctions; both are fcc with a lattice parameter of 5.24 Å. It is also shown that this fcc phase is stabilized by the presence of significant quantities of oxygen. The possible effects of thin foil preparation by ion milling techniques in producing the observed bcc phase is also briefly discussed.

INTRODUCTION : The microstructure of Nd-Fe-B, a recently developed[1,2] hard magnetic alloy system, is being intensively investigated to understand the magnetization reversal mechanism responsible for the changes in coercivity caused by thermal treatments[3-6]. Of particular interest is the structure and composition of phases present at the grain boundaries of the main magnetic phase, $Nd_2Fe_{14}B$, since the nucleation and pinning events responsible for coercivity are thought to occur at these boundaries[7,8]. There have been several investigations aimed at explaining the microstructural features observed along the grain boundaries[9-12]. Previous results using microdiffraction proved the existence of a fcc phase at the grain boundaries[13]. However further clarification of the structure and composition of the phase(s) present is needed. Thus, the objective of this paper is to clarify some of these aspects, by electron microscopy, microanalysis, and Auger spectroscopy. Also, the possible influence of specimen preparation techniques on the microstructures observed will be briefly discussed.

EXPERIMENTAL : The sintered magnets were produced by standard processing techniques, as described in reference 11. The alloy studied in this investigation had a nominal composition of Fe-33.5 w/o Rare Earth - 1 w/o B with a rare earth composition of 79.6% Nd/16.8% Pr/ 3.6% Ce. The magnets were examined in the optimally treated condition, consisting of quenching the sample from the sintering temperature, followed by annealing for one hour at 600°C. A ternary Fe-32 w/o Nd-1.4 w/o B alloy was also examined for comparison. Electron thin samples were prepared by mechanically thinning a 500 micrometer thick foil to about 75-100 micrometers, followed by Argon ion milling to electron transparency. Foils were also prepared by jet polishing using a 20:1 ethanol / perchloric

acid mixture at $0^{o}C$. The samples were examined using a Philips 400 TEM/STEM at 100 kV and a JEOL 200CX at 200 kV. The JEOL 200CX was fitted with an ultra-thin window Energy Dispersive X-ray (EDX) detector that enabled the detection of elements with atomic number greater than or equal to six. Microanalysis was carried out using the theoretical k-factors from the system software. Experimental k-factors were measured using the matrix phase, $Nd_2Fe_{14}B$, in order to check the validity of the quantification using theoretical k-factors. For Auger spectroscopy, samples were 7 fractured in-situ under a vacuum of 3×10^{-9}torr. In addition to point analyses, Auger electron maps were also generated to examine the distribution of the elements.

RESULTS : Further microanalysis experiments by tilting through various orientations substantiated our previous conclusions that the grain boundary phase is indeed fcc. Fig.1 shows the general microstructure of the magnet. Fig.1(a) depicts the triple grain junction phase, and is schematically described in Fig.1(c). Fig.1(b) depicts the two-grain boundary phase and is schematically described in Fig.1(d). The crystal structure of the three-grain junction phase has been elucidated in an earlier paper to be fcc[13]. The phase at the two-grain boundaries is generally 200-300 Å in width. Hence, several regions were examined before selecting a region which was thick enough to obtain microdiffraction and analytical information using a 400 Å size probe. Fig.2 shows a typical bright field image of one such region. The inset shows microdiffraction patterns from different regions along the two-grain boundary, all of which can be indexed as $[110]_{fcc}$, thus indicating that the two-grain boundary region is an extension of the single crystal three-grain junction region. Two grain boundary regions with polycrystalline films also occur.

Preliminary EDX microanalysis of the triple grain junction region using a conventional Beryllium window EDX detector indicated a composition that was rich in the rare earths, but contained significant amounts of Fe. Quantification led to a composition of 70-75 a/o rare earth and 25-30 a/o Fe. However, examination of the Fe-Nd binary phase diagram[14] indicated no fcc phase in this composition range. Preliminary experiments using an ultra-thin window EDX detector indicated[13] significant amounts of oxygen present in this fcc phase. Subsequent experiments conclusively proved that this phase did contain oxygen. Fig.3 is the low energy end of of the EDX spectrum, depicting the oxygen peak. Quantification has been carried out with the thin foil approximation using the theoretical k-factors from the system software. The results indicate oxygen contents varying from 20-50 a/o. This large variation in the oxygen content can be attributed to two reasons : (1) the soft oxygen x-rays are absorbed by the Nd, leading to a reduced x-ray intensity peak for oxygen, which is strongly dependent upon the foil thickness and density of the material. Experiments are now underway to accurately measure the foil thickness to account for this absorption. In spite of this uncertainty in quantification, the oxygen content calculated is a lower limit to the amount actually present in the area. (2) The actual oxygen content does indeed vary greatly from region to region, depending on processing conditions. One significant aspect is that, within the limits of experimental error (~10%), the two grain boundary region has the same composition as the triple grain junction region. Fig.4 is an EDX spectrum of the two regions, showing the similarity in composition.

The presence of oxygen in the grain boundary phase was independently confirmed by Auger spectroscopy of in-situ fractured surfaces. Elemental distributions were determined by first generating elemental Auger maps. Fig.5 shows a typical fracture surface and the corresponding

oxygen-Auger map from which the segregation of oxygen to the grain boundaries as well as to the grain surfaces can be resolved. Using the map, regions of oxygen enrichment were then isolated for point analyses. Fig.6 shows a typical Auger spectrum from a oxygen rich area. There are several features of interest in this spectrum. First, there is a large amount of oxygen present, which corroborates the EDX results obtained using thin foils. Second, there is no detectable boron in this grain boundary phase. Finally, this phase is Neodymium rich, with smaller amounts of iron. Such a spectrum was consistently obtained from oxygen rich regions.

The oxygen and rare earth distribution is not uniform in the triple grain junctions. Fig.7 shows schematically the point analyses across a triple grain junction region. The results for the ternary Nd-Fe-B alloy are shown in Fig.8. It can be seen that oxygen tends to segregate to the center of the junction. Similar results were obtained with Ce-Pr-Nd samples also. Fig.9 shows the point analysis across one such triple grain junction region in a 79.6% Nd/16.8% Pr/ 3.6% Ce sample. It is clear that oxygen segregates to the center of the region, while Ce and Pr appear to segregate to the interfaces.

<u>The bcc phase</u> : In several instances, a bcc phase with a lattice parameter of 2.9 Å has been observed at the grain boundaries of the $RE_2Fe_{14}B$ grains. The low coercivity in the as-quenched condition has been attributed to the presence of bcc platelets extending into the matrix from the grain boundaries, deforming the lattice of the $RE_2Fe_{14}B$ grains[9,10,11]. It has also been observed that these platelets disappear on annealing at 600°C, and several researchers have suggested that this transformation is the cause for the large increase in coercivity observed after such a treatment. The bcc phase, in all reported cases, has been observed by the

Selected Area Diffraction (SAD) technique, using Argon ion-milled specimens. SAD using a 0.5 micrometer aperture has been carried out on Argon ion milled specimens. When the SAD aperture is placed over the matrix only, a bcc ring pattern with a lattice parameter of 2.9Å is observed, Fig.10(a). Fig.10(b) is the dark field image of the same region using the $(110)_{bcc}$ ring, showing the dispersed, inhomogeneous nature of this phase. When the SAD aperture is placed over the grain junction region alone, the bcc ring pattern is not observed, as shown in Fig.11. It may also be pointed out that while the foil thickness is changing, the dispersed bcc regions are uniformly distributed, indicating that the bcc regions are not internal to the sample.

Discussion : (1) The fcc phase: The fcc phase at the two grain boundaries and three grain junctions have the same composition and lattice parameter, suggesting that the two grain boundary region is an extension of the fcc phase existing at the triple grain junctions. From Figs.3 & 4 it is clear thar this phase is stabilized by significant amounts of oxygen. This phase is consistent with a NdO type oxide that has a NaCl structure with lattice parameter 5.09Å[14]. The presence of oxygen is explained by the large affinity of the rare earths for oxygen. This affinity coupled with the formation of fine powders during ball milling causes oxidation of the particle surfaces. From the Auger map it is clear that oxygen exists not only at the grain junctions, but also at the interfaces of two grains. It is also clear from the Auger spectra that there is no detectable amount of boron in the grain boundary phase, which could be stabilizing an otherwise unstable structure. Furthermore, the presence of oxygen in the liquid phase ensures that its eutectic decomposition to ß-Nd + Nd_2Fe_{17}[15] does not take place. It should be pointed out that Nd_2Fe_{17} is a soft magnetic

phase, and if formed at the grain boundaries, could lead to a degradation in coercivity. As seen from Figs. 7 and 8, the oxygen distribution is not uniform across a triple grain junction. While the oxygen concentration is higher in the center of the region, Ce and Pr appear to have segregated to the interfaces. This distribution may be indicative of the various processes taking place during liquid phase sintering and is currently under investigation.

(2) The bcc phase: The observation of a bcc phase, both at the grain boundaries as well as in the interior of the grains requires detailed investigation. This is all the more significant since platelets of the bcc phase have been attributed to be the cause for a low coercivity. However, in the present work, it is suggested that the bcc phase, especially that observed in the intra-granular region, is produced by a re-deposition process during ion-milling for thin foil preparation. This argument is supported by the fact that the density of the particles is uniform although the foil thickness is changing. The process of re-deposition is elucidated schematically in Fig.12. In (a), a thin foil is shown as a slab, for simplicity. In this slab, there exists a grain boundary region of thickness 200-300Å. This phase is softer than the matrix and hence mills faster. Thus, at an intermediate stage during ion-milling, the foil can be represented schematically as in (b). Here, a "valley" is formed at the grain boundary due to the faster milling rate of the fcc phase. During ion-milling, the milled debris, instead of depositing elsewhere in the machine, deposits on the surface of the foil. Since the foil is rich in Fe, at temperatures below 700°C the debris takes the structure most suitable for such a high concentration of Fe, i.e., bcc with a lattice parameter of 2.9Å. It may be pointed out that this observation, by itself, does not rule out the presence of a truly structural bcc phase at the grain boundaries, in addition to the fcc phase. Hence, it can only be concluded that a bcc phase

" may or may not" exist at the grain boundaries. Since it is essential to understand the detail nature of this phase in order to elucidate the causes for changes in coercivity, the presence or absence of this phase has to be verified by other independent experiments, such as jet polishing. Such experiments have been carried out and preliminary results are presented here. Fig.13 is a dark field image of the grain boundary region of the Fe-Nd-B magnet, imaged with the (111) and (200) rings of the resulting fcc pattern. Note the continuous nature of the phase throughout the grain boundary. This result tends to support our proposal that the bcc phase is indeed an artefact in the alloys investigated. Further investigations are underway to verify this.

CONCLUSIONS: In conclusion, it has been shown that the grain boundary phase, both at the triple grain junctions[13] as well as in the two-grain boundaries, is face centered cubic. This structure is stabilized by the presence of significant amounts of oxygen, which is present as a result of processing steps. The presence of oxygen was established with the use of an ultra-thin window Energy Dispersive X-ray detector. In addition, this phase contains some dissolved Fe. It is thought that the bcc phase observed, especially in the intra-granular regions, is a ion-milling artefact.

ACKNOWLEDGEMENTS : The authors gratefully acknowledge Prof. M.Okada, Tohuku University, Japan, and W.Rodewald, Vacuumschmelze, West Germany, for kindly providing the alloys used in this study. This work was supported by the Director, Office of Basic Energy Research, Office of Basic

Energy Sciences, Materials Science Division of the US Department of Energy under contract No.DE-AC03-76SF00098.

REFERENCES

1. M. Sagawa, S. Fujimura, N. Togawa, H. Yamamoto and Y. Matsuura, J. Appl. Phys. 55, 2083 (1984).
2. J. F. Herbst, J. J. Croat, F. E. Pinkerton and W. B. Yelon, Phys. Rev. B, 29, 4176 (1984).
3. M. Sagawa, S. Fujimura, H. Yamamoto, Y. Matsuura and K. Hiraga, IEEE Trans. Magnetics, MAG-20, 11584 (1984).
4. J. D. Livingston, 8th International Workshop on Rare Earth Permanent Magnets and their Applications, K. Strnat ed., University of Dayton, School of Engineering, Dayton, Ohio 45469, 423 (1985).
5. K. D. Durst and H. Kronmuller, 8th International Workshop on Rare Earth Permanent Magnets and their Applications, K. Strnat ed., University of Dayton, School of Engineering, Dayton, Ohio 45469, 725 (1985).
6. K. S. V. L. Narasimhan, J. Appl. Phys. 57, 4081 (1985).
7. R. K. Mishra, J. K. Chen and G. Thomas, J. Appl. Phys. 59, 2244 (1986).
8. G. C. Hadjipanayis, K. R. Lawless and R. C. Dickerson, J. Appl. Phys. 57, 4097 (1985).
9. K. Hiraga, M. Hirabayashi, M. Sagawa and Y. Matsuura, Japanese J. Appl. Phys. 24, 699 (1985).
10. M. Sagawa, S. Fujimura, H. Yamamoto, Y. Matsuura S. Hirosawa and K. Hiraga, 8th International Workshop on Rare Earth Permanent Magnets and their Applications, K. Strnat ed., University of Dayton, School of

Engineering, Dayton, Ohio 45469, 587 (1985).

11. K. Hiraga, M. Hirabayashi, M. Sagawa and Y. Matsuura, Japanese J. Appl. Phys. 24, L30 (1985).

12. N. A. ElMasry and H. H. Stadelmaier, Materials Letters, 3, 405 (1985).

13. R. Ramesh, K. M. Krishnan, E. Goo, G. Thomas, M. Okada and M. Homma, Journal of Magnetism and Magnetic Materials, 54-57, 563 (1986).

14. K. A. Gschneidner, Rare Earth Alloys, (D. Van Nostrand Company, Inc., Princeton, New Jersey, 1961).

15. Handbook of Binary Phase Diagrams, Vol.3, Ed. W.G.Moffatt, General Electric Company, Business Growth Services, 120 Erie Boulevard, Schnectady, New York 12305, USA., (1978).

Figure Captions

Fig. 1. General bright field microstructure of the magnet depicting the grain boundary phase at the (a) triple grain junction and (b) two grain boundaries. (c) and (d) respectively depict (a) and (b) schematically.

Fig. 2. Bright field image of the two grain boundary region along with its microdiffraction pattern showing the [110] fcc structure.

Fig. 3. Low energy end of the EDX spectrum from the triple grain junction indicating the presence of oxygen.

Fig. 4. EDX spectra from the triple grain junction and adjacent two grain boundary showing the identical composition of these two regions.

Fig. 5. (a) Fracture surface of an in-situ fractured sample, and (b) the corresponding oxygen-Auger map.

Fig. 6. Auger point analysis from an oxygen rich region depicting significant oxygen and neodymium concentrations, along with smaller iron concentrations. Note the absence of boron.

Fig. 7. Schematic illustration of successive EDX point analyses across a triple grain junction region. The diameter of the spots indicate the approximate probe size.

Fig. 8. Composition profile across the triple grain junction for a ternary Nd-Fe-B alloy.

Fig. 9. Composition profile across the triple grain junction for a [Ce-Pr-Nd]-Fe-B alloy.

Fig. 10. (a) Bright field image and the corresponding SAD pattern of the matrix region showing the presence of a bcc phase. (b) Dark field image using the 110 bcc ring showing the inhomogeous bcc phase.

Fig. 11. Bright field image of the triple grain junction along with the corresponding SAD pattern. Note the absence of any bcc ring pattern.

Fig. 12. Schematic illustration of the formation of the bcc phase by re-deposition during ion milling. (a) Starting foil configuration. (b) Foil after milling for some time. (c) Final foil configuration showing the bcc surface layer.

Fig. 13. Dark field image of the two grain boundary region from a jet electropolished sample using the 111 and 200 fcc rings.

0.2 μm
(a)

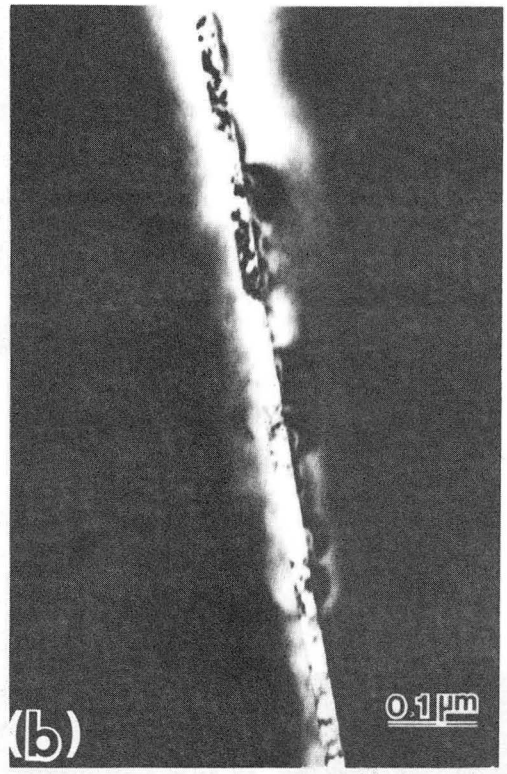
0.1 μm
(b)

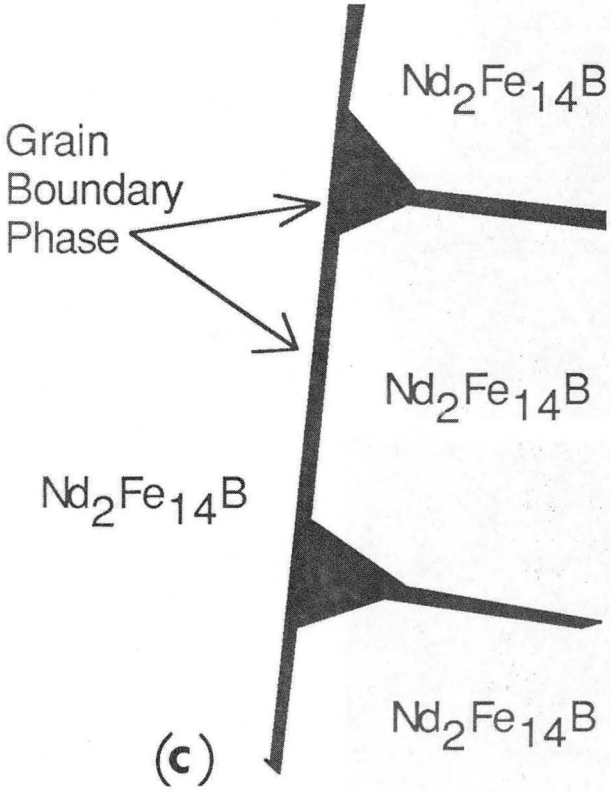
Grain
Boundary
Phase
$Nd_2Fe_{14}B$
$Nd_2Fe_{14}B$
$Nd_2Fe_{14}B$
$Nd_2Fe_{14}B$
(c)

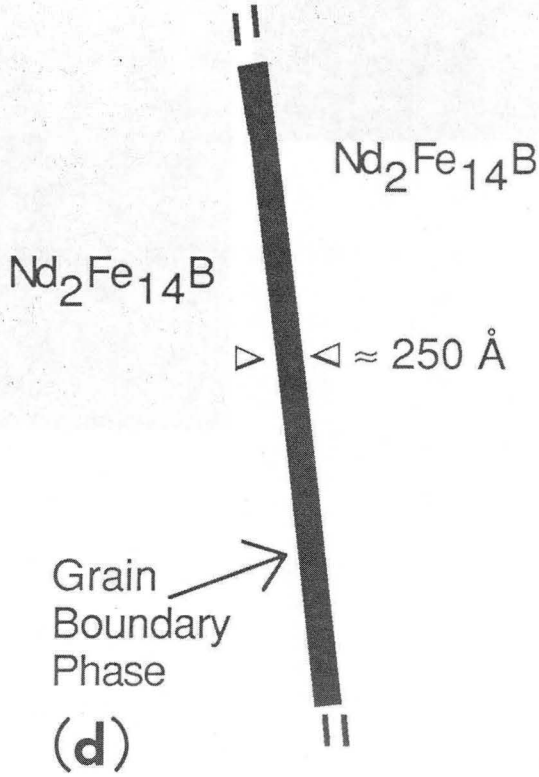
$Nd_2Fe_{14}B$
$Nd_2Fe_{14}B$
≈ 250 Å
Grain
Boundary
Phase
(d)

XBB 862-1270

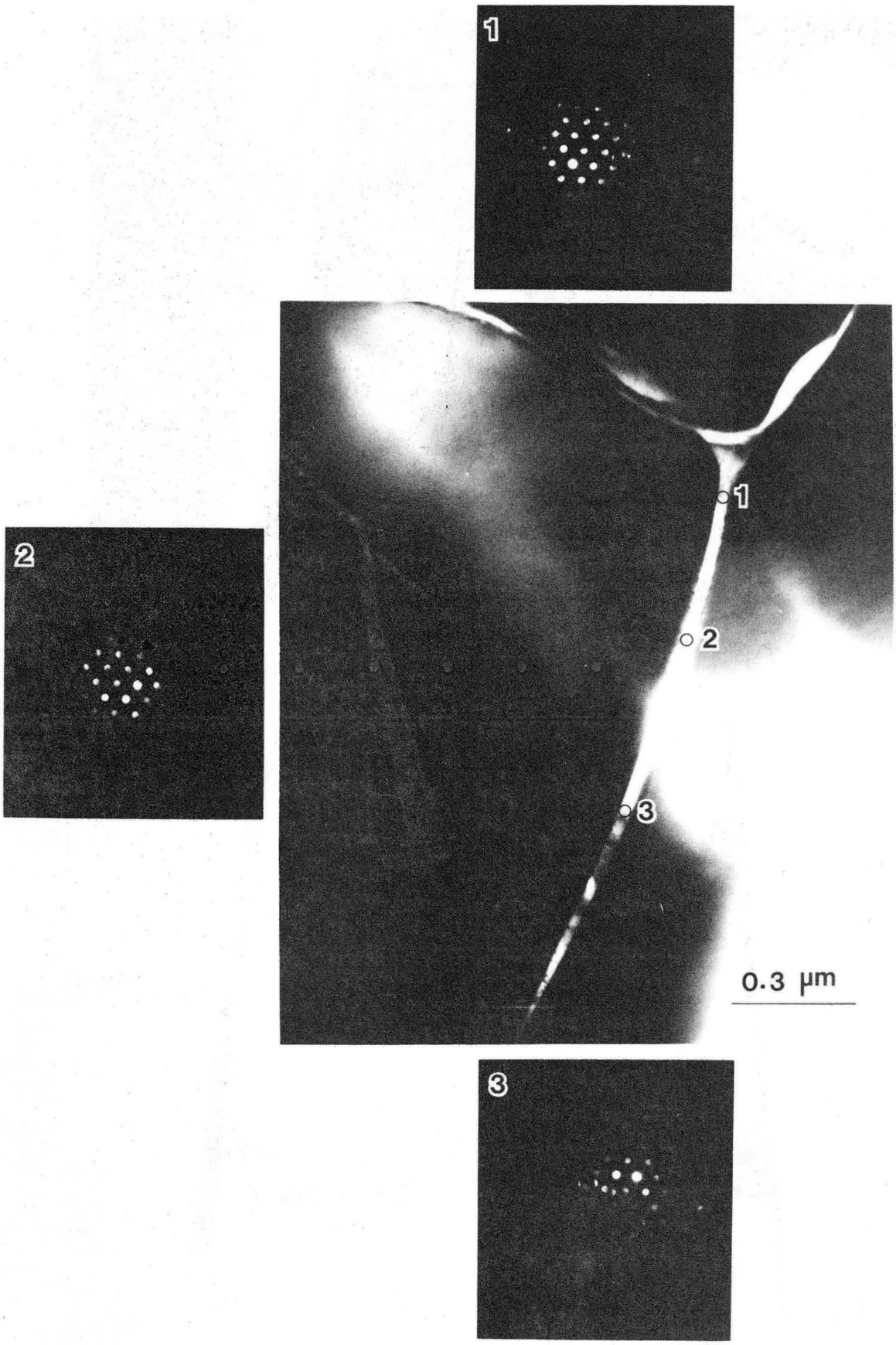

XBB 865-3634

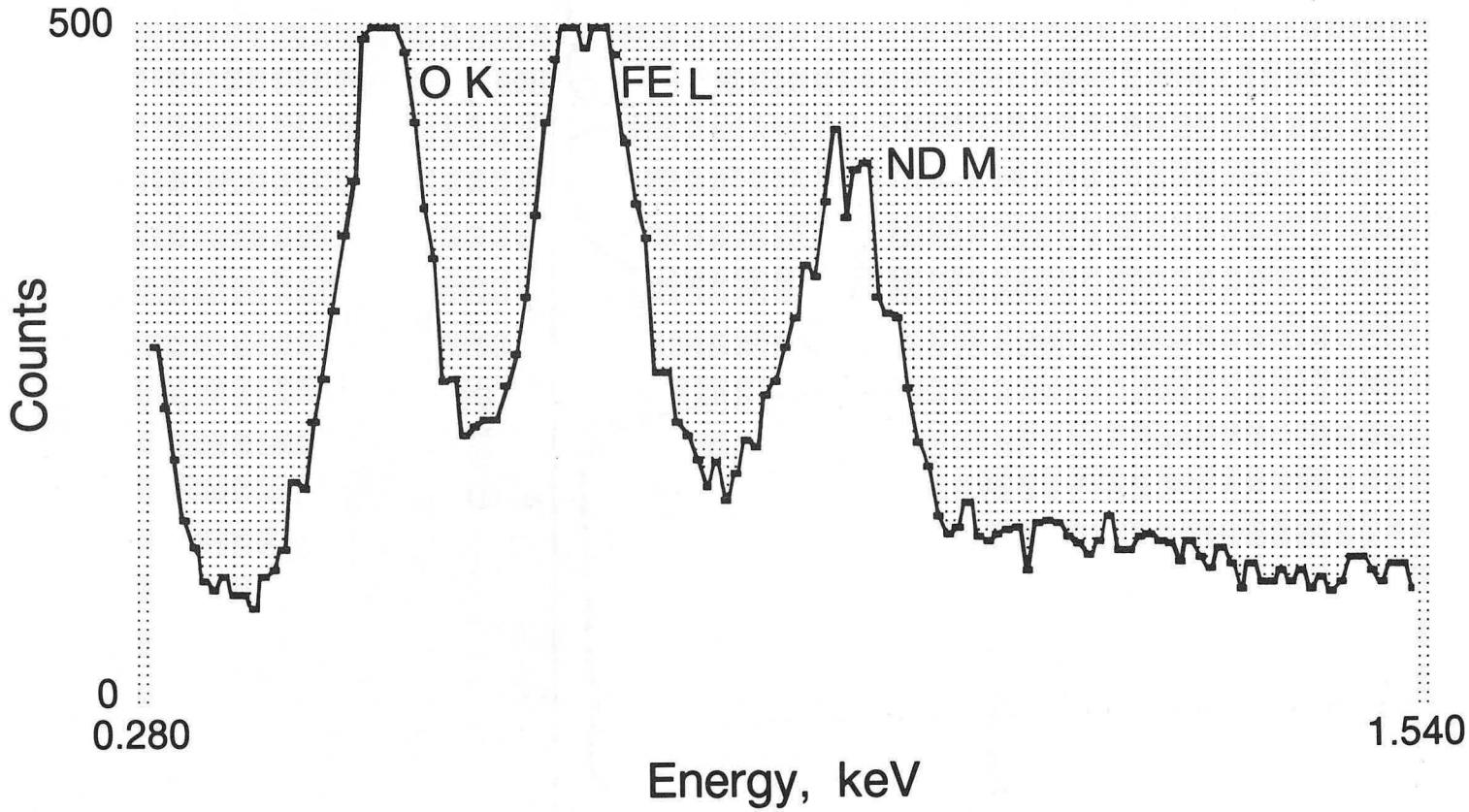

XBL 862-634A

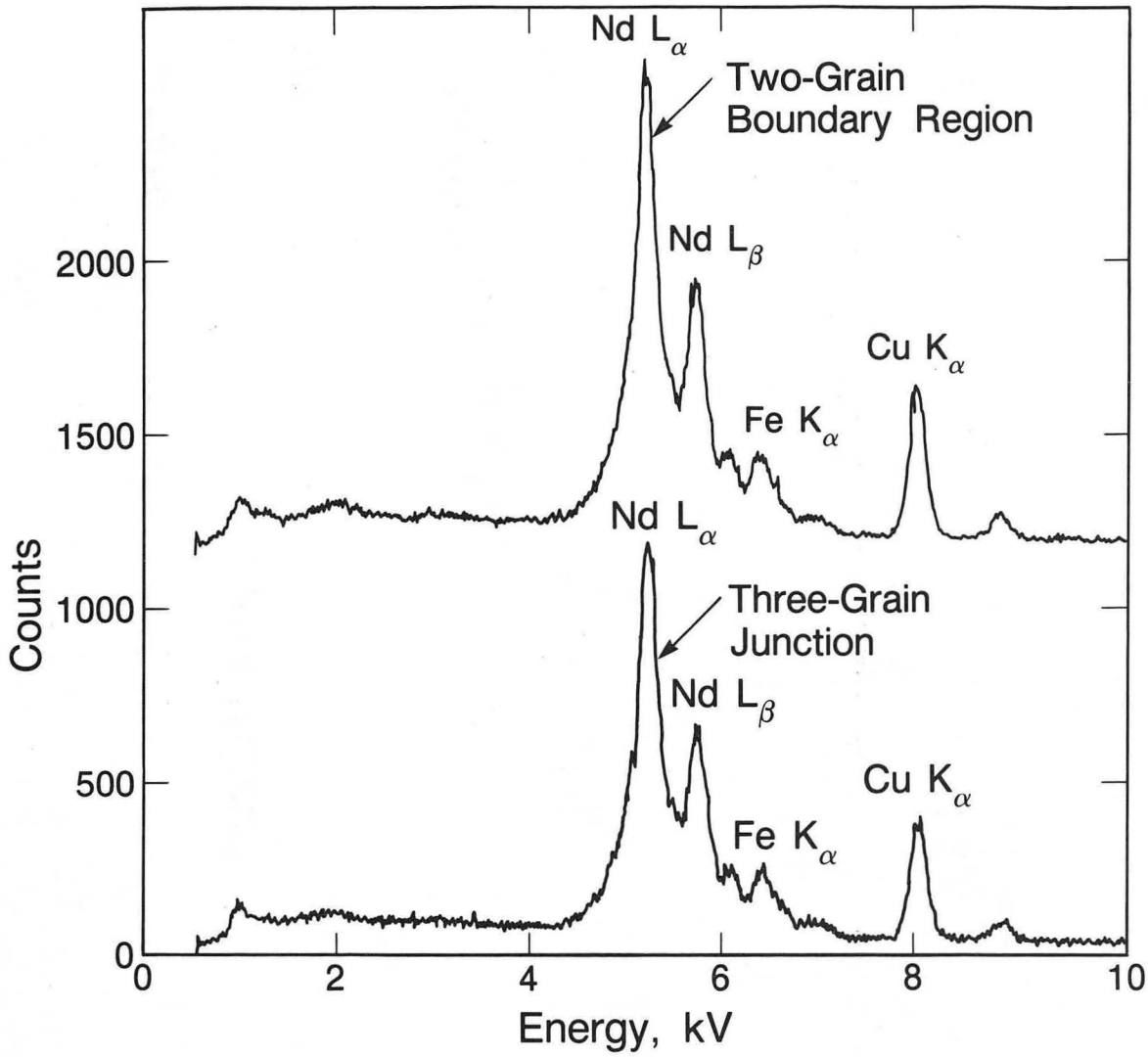

XBL 8611-9025

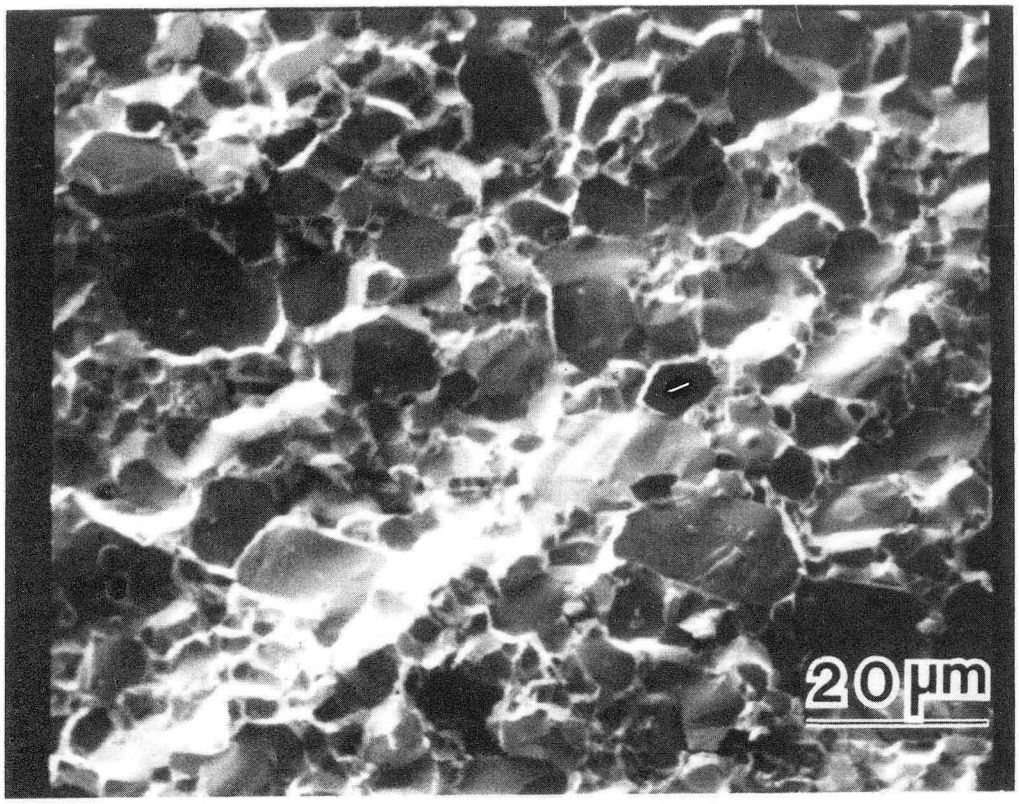

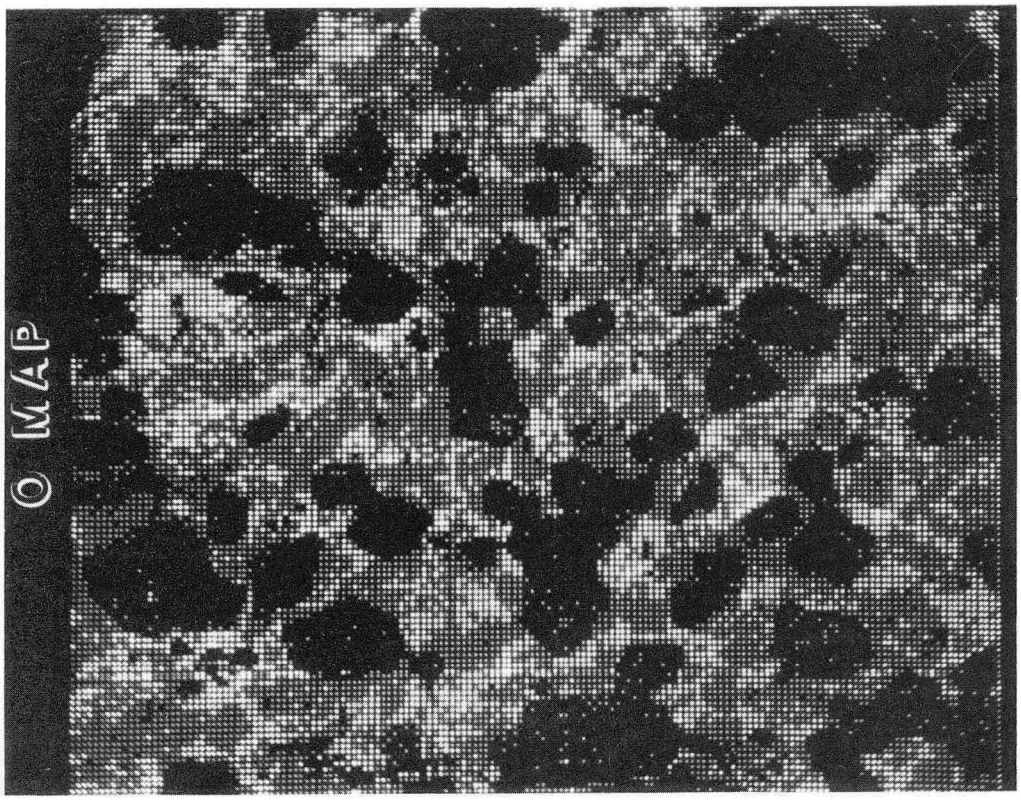

XBB 850-10301

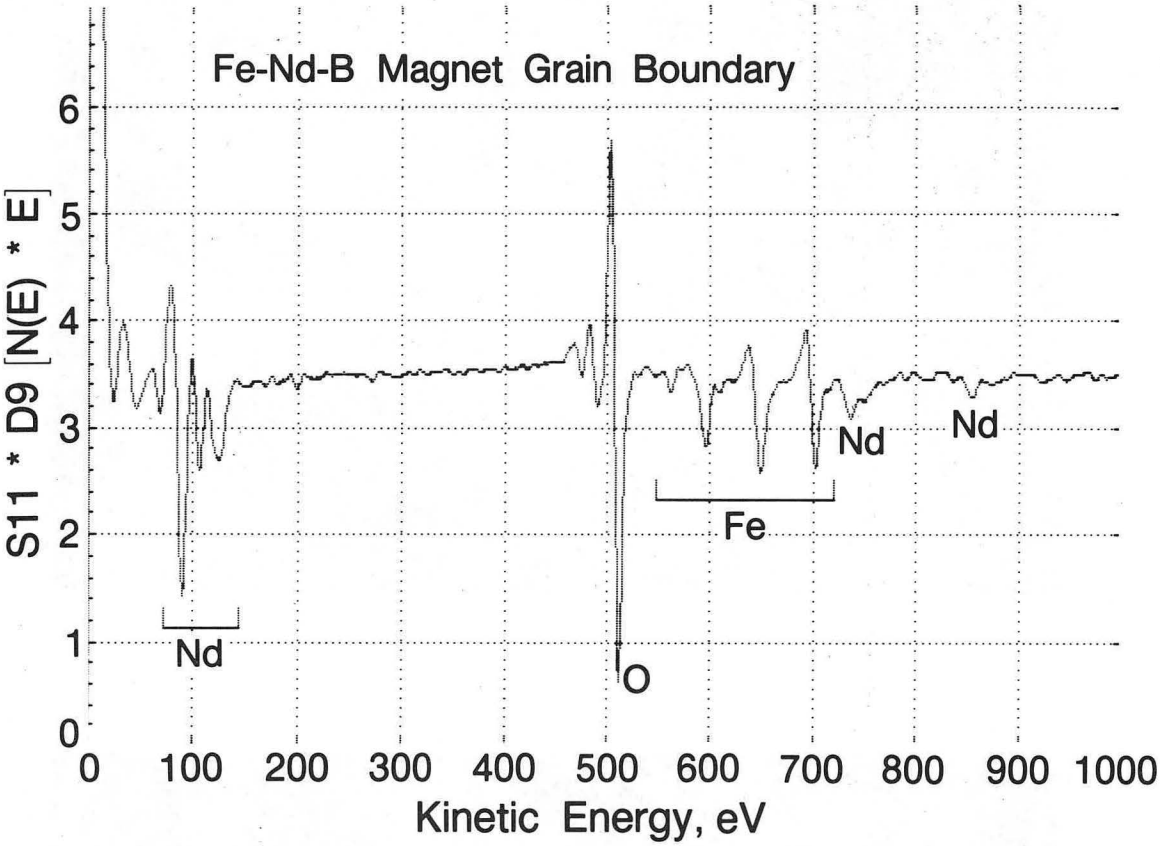

XBL 859-3984A

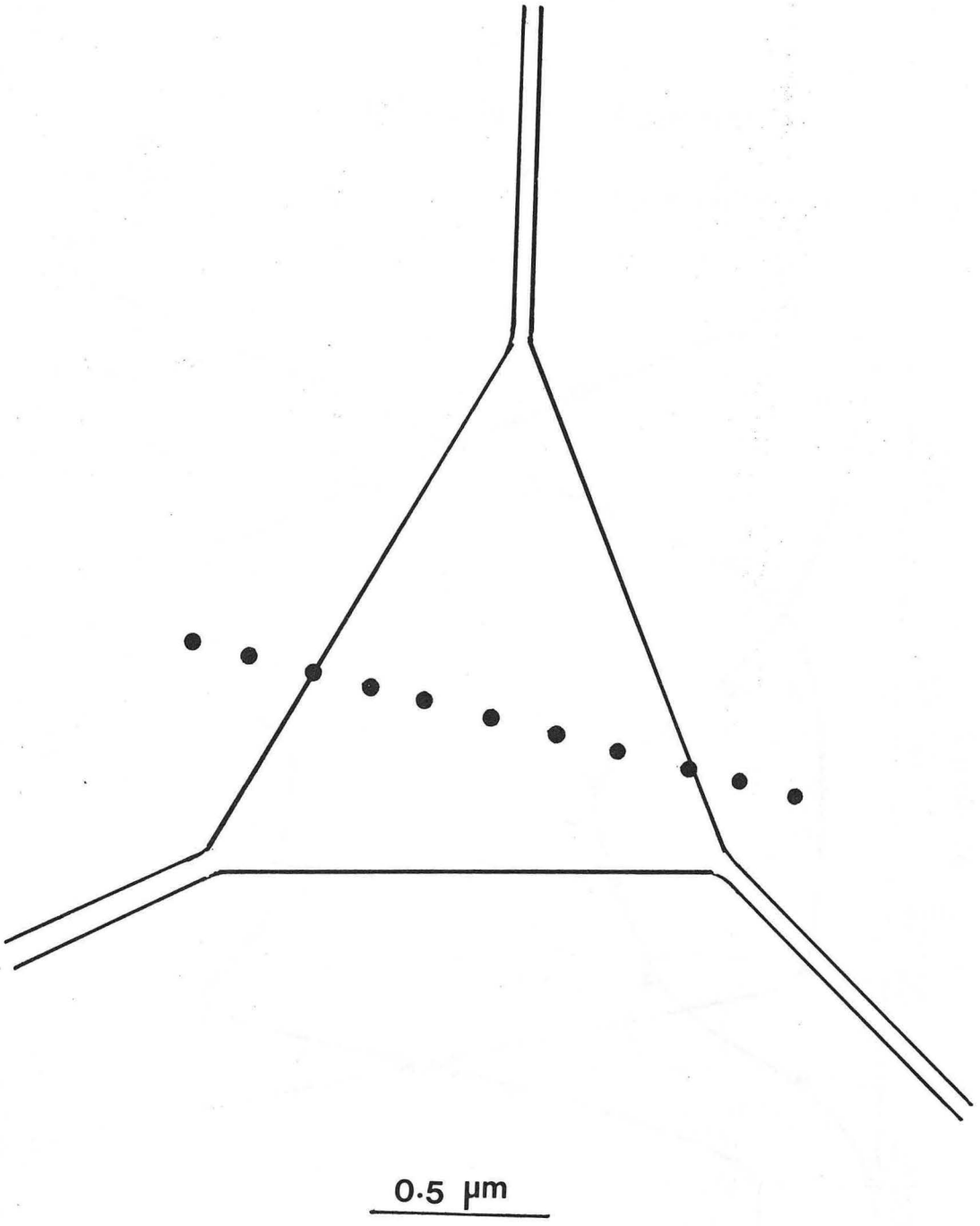

XBL 868-2980

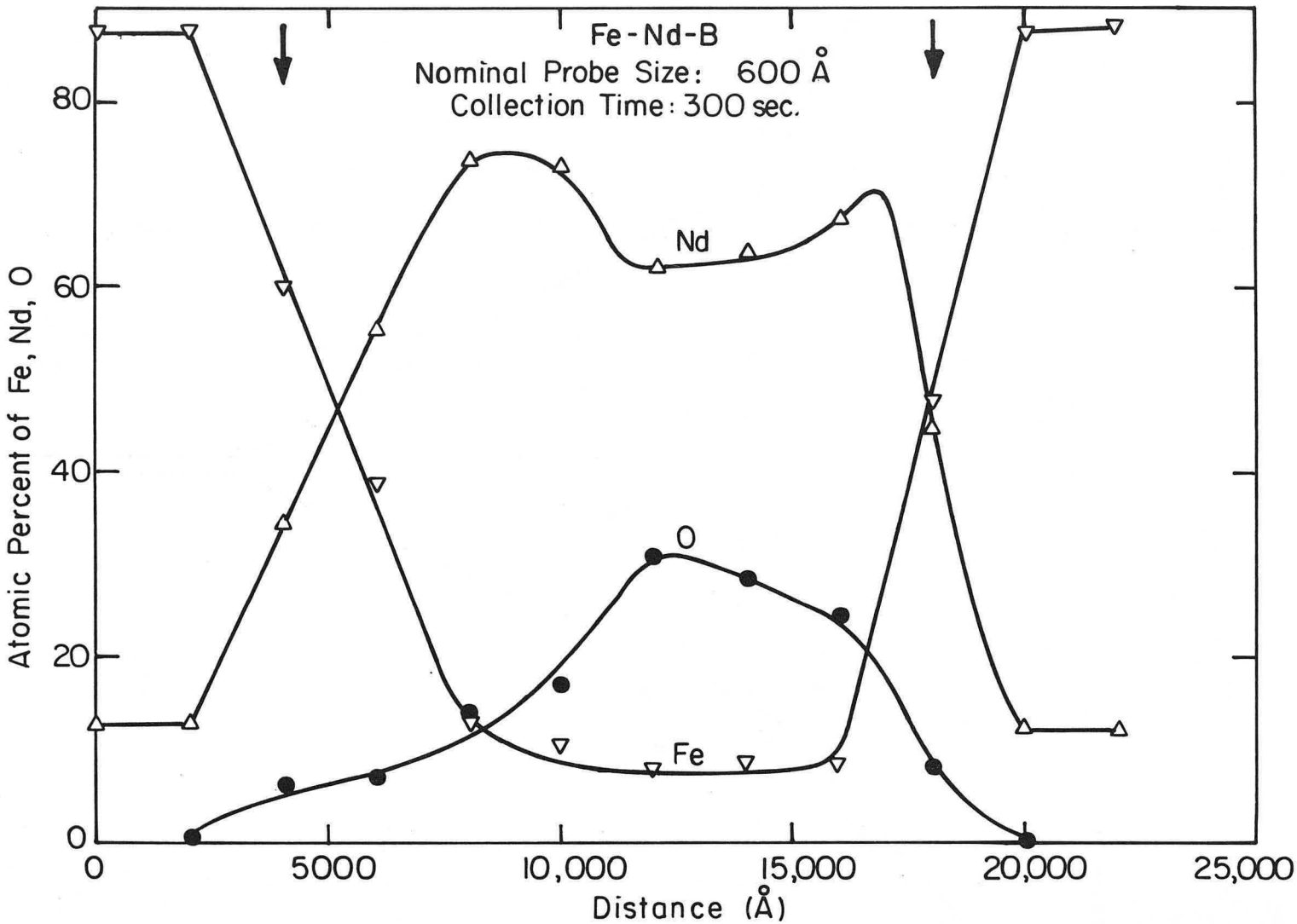

XBL8510-6756

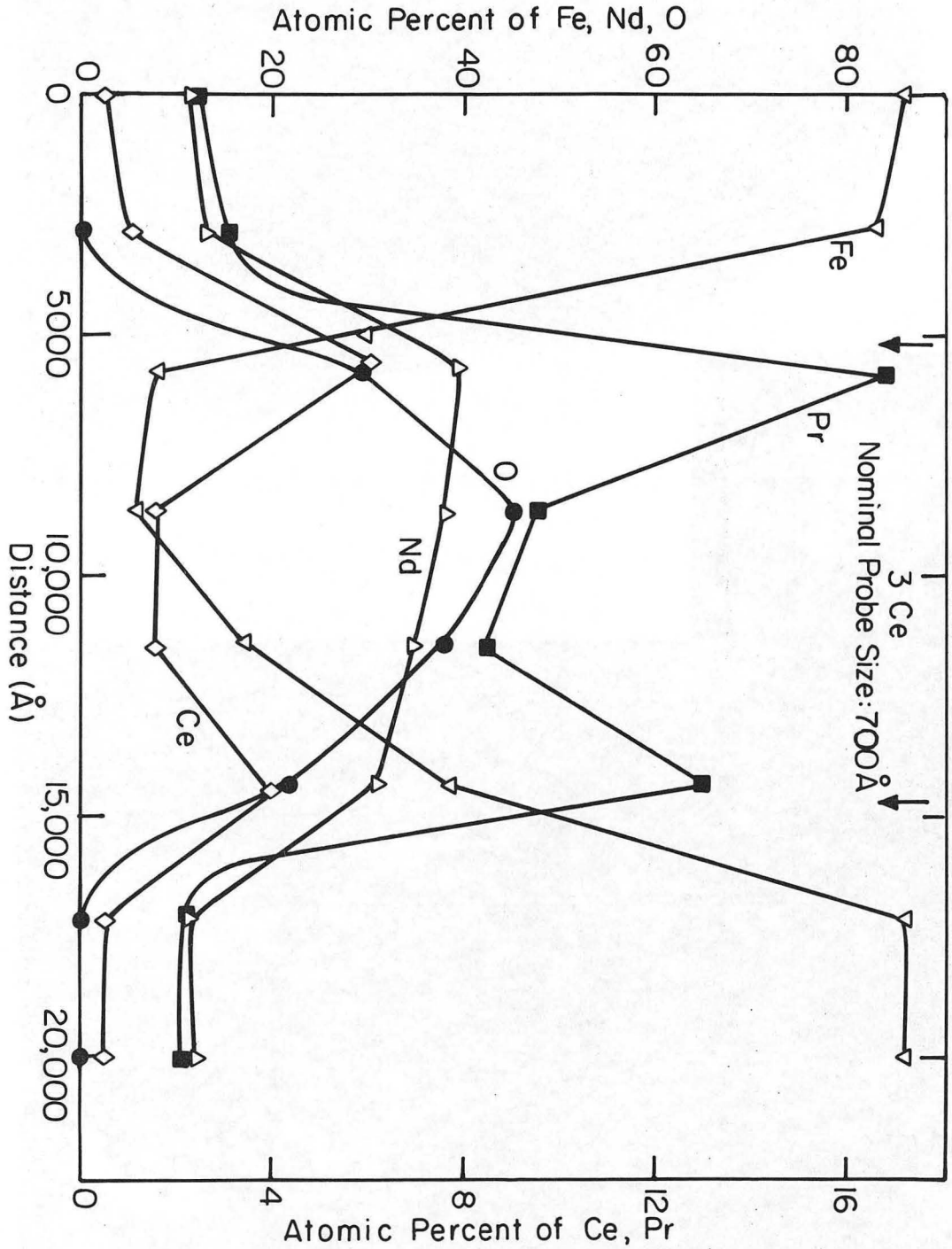

XBL 8510-6757

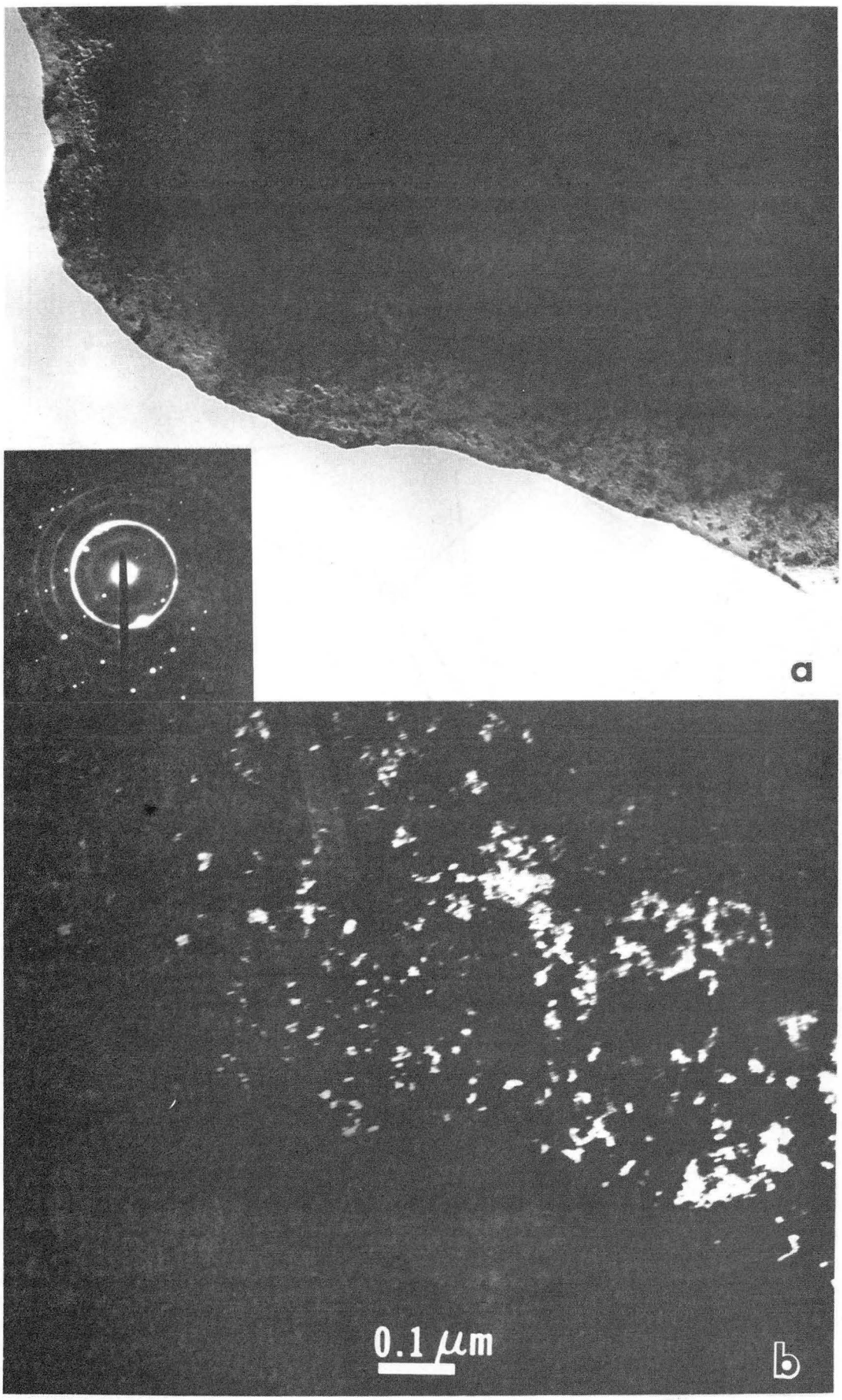

XBB 867-5985

XBB 868-6264

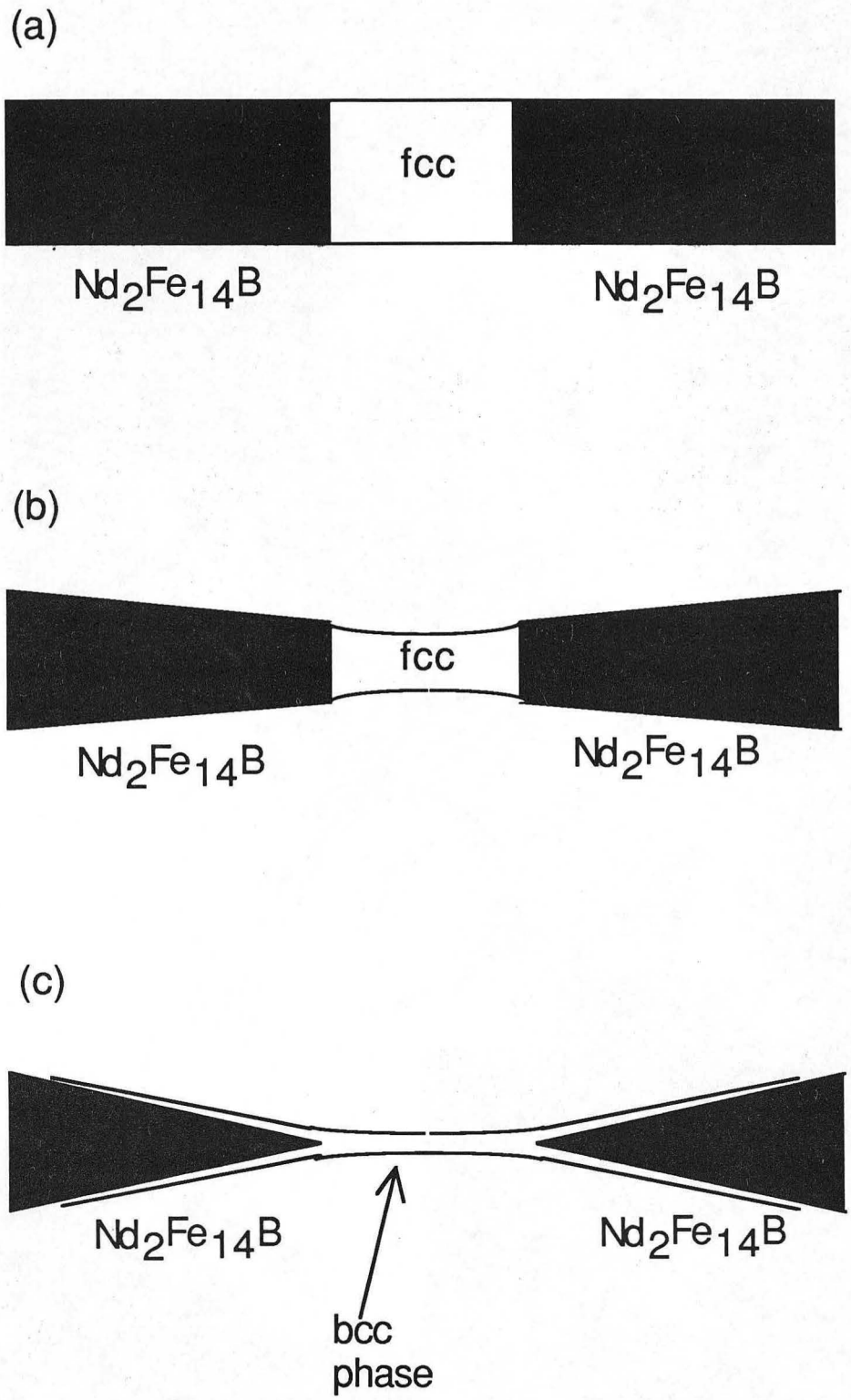
(a)
fcc
$Nd_2Fe_{14}B$
$Nd_2Fe_{14}B$
(b)
fcc
$Nd_2Fe_{14}B$
$Nd_2Fe_{14}B$
(c)
$Nd_2Fe_{14}B$
$Nd_2Fe_{14}B$
bcc
phase

XBL 868-3206

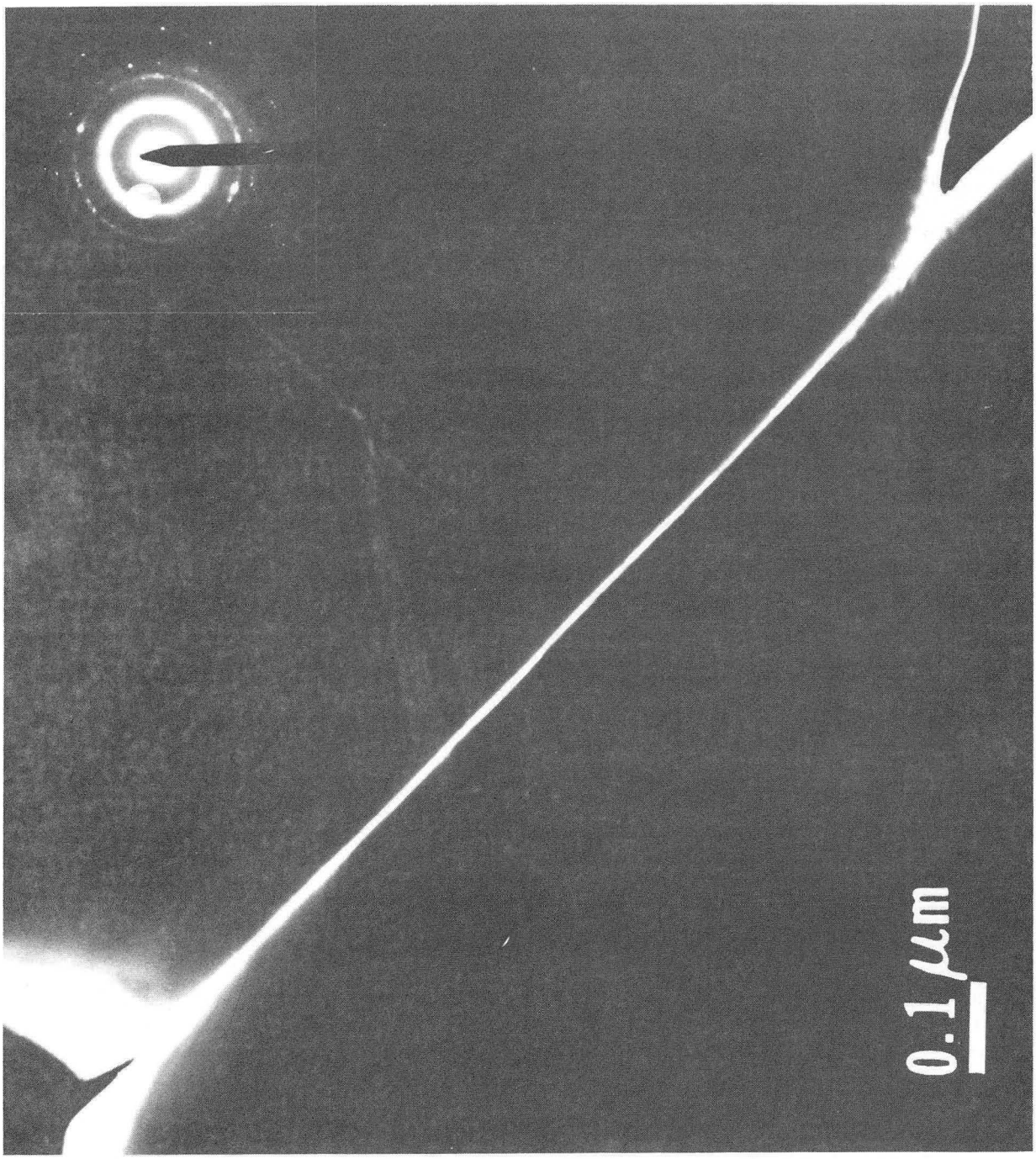
0.1 μm

This report was done with support from the Department of Energy. Any conclusions or opinions expressed in this report represent solely those of the author(s) and not necessarily those of The Regents of the University of California, the Lawrence Berkeley Laboratory or the Department of Energy.

Reference to a company or product name does not imply approval or recommendation of the product by the University of California or the U.S. Department of Energy to the exclusion of others that may be suitable.

LAWRENCE BERKELEY LABORATORY
TECHNICAL INFORMATION DEPARTMENT
UNIVERSITY OF CALIFORNIA
BERKELEY, CALIFORNIA 94720